Landslide at Orleans, Ontario

Eden, W. J.; Jarrett, P. M.

Publisher's version / Version de l'éditeur:
https://doi.org/10.4224/20373789
Technical Paper (National Research Council of Canada. Division of Building Research), 1971-03

LANDSLIDE AT ORLEANS, ONTARIO

by W. J. Eden and P. M. Jarrett

Ottawa
Price 50 cents

March 1971
NRCC 11856

GLISSEMENT DE TERRAIN A ORLEANS, ONTARIO

RESUME

L'étude de glissements de terrain dans la région d'Ottawa a révélé que l'argile qui a créé le manquement n'était pas une argile intacte, mais plutôt une argile comprenant un réseau de petites fissures. Cette communication traite de l'étude d'une pente de route, haute de 35 pieds, qui a glissé cinq ans après la construction. Un rapport étroit a été obtenu entre les faits observés et les résistances mesurées lors des essais en laboratoire en utilisant l'appareil triaxial avec faibles contraintes sur l'éprouvette.

NATIONAL RESEARCH COUNCIL OF CANADA
DIVISION OF BUILDING RESEARCH

LANDSLIDE AT ORLEANS, ONTARIO

by

W. J. Eden and P. M. Jarrett

Technical Paper No. 321
of the
Division of Building Research

Ottawa
March 1971

LANDSLIDE AT ORLEANS, ONTARIO

by

W. J. Eden and P. M. Jarrett

ABSTRACT

Studies of landslides in the Ottawa area have indicated that the clay involved in the failure was not an intact clay, but one containing a system of fissures. This paper deals with one of the cases studied, in which a 35 ft cut slope for a roadway failed five years after construction. Good agreement was achieved between the strength derived from the field study and the strength measured in the laboratory using the triaxial apparatus with low confining stresses.

DESCRIPTION OF SLIDE

On 10 October 1965, a small landslide occurred in the side hill cut of a road from a housing subdivision at Orleans, Ontario. The road descended from a 50-ft high clay terrace to the former route of Highway 17 at the toe of the slope. Figure 1 is a plan of the area showing the terrace and the alignment of the road, which was constructed in 1960. To achieve a maximum gradient of 10%, a side hill cut of varying depth was necessary. The slopes of the side hill cut were a constant source of trouble due to surface sloughing. At the location of the landslide, the cut slope was inclined at nearly 35°.

The initial slip occurred at 8.30 a.m. following a period of heavy rainfall (1.4 in. in the three preceding days). The slip involved the total height of the slope, and covered the road with debris. Figure 2 shows a view of the crater, after the spoil had been removed from the roadway. Figure 3 is a plan of the landslide prepared from stereoscopic photographs.

Numerous tension cracks which remained around the perimeter of the first slide were involved in a second slide two weeks later on 23 October 1965. This slide occurred during a heavy rain (1.14 in. overnight) and extended the crater of the first slide (see Figure 3). Figure 4 shows the tension cracks at the top of the slope preceding the second slide. It is apparent that hydrostatic pressure acting in the cracks initiated the second slip. Figure 5 is a view of the crater after the second slide. Debris from this slide also spilled onto the roadway.

After the first slide, a narrow tension crack was observed running along the cut face to the south of the crater (Figure 3). After the second slide, a vertical movement of about 2 ft was noticed between the ground level on one side of the crack relative to the other. The crack (Figure 6) was about 3 in. wide. Another slide was considered to be imminent but in spite of frequent rainfalls, failure did not occur. Between December and February 1966, a third slide occurred below the crack but it was confined to the cut face and failed well above the toe of the slope. When the road was repaired, some spoil material was placed at the toe of the slope. The stabilizing effect of this material is evident because the third slide failed above the fill material and slid over it.

FIELD WORK

Field work began immediately after the first slide. Surveys were taken of the crater and immediate area. Through the cooperation of the Photogrammetry Section of the Division of Applied Physics, stereoscopic photographs with a photo theodilite were used for preparation of a detailed plan (Figure 3). It is believed that the failure plane passed through the toe of the slope, since a culvert passing under the road just beyond the toe was left intact. In the upper region of the failure, very little debris obscured the failure surface. The lower regions were probed with a hand auger and the failure surface was established (see Figure 7, a profile of the slide).

Shortly after the first slide, piezometers 0_1 and 0_2 were installed to the south of the crater, and vane test No. 1 was carried out at the location shown on Figure 3.

After the second slide, a survey was made of the extended crater. Two more piezometers (0_3 and 0_4) were installed. Vane test No. 2 was made and undisturbed samples were taken at locations shown on Figure 3. The samples were taken continuously from a depth of 4 ft to 49 ft using a 54 mm N.G.I. fixed piston sampler. The samples revealed that the terrace was made up of clay, with some layers of silt or fine sand. A year after the slide, samples were obtained from borings 2 and 3 made on either side of the crater. The main purpose of these borings was to check on the continuity and elevation of the silt layers.

Piezometer readings have been continued at the site, with frequent readings being taken in exceptionally wet periods. The object of these observations was to try to establish the piezometric regime existing at the time of the slide. In November 1966 piezometer 0_1 was removed and reinstalled at the toe of the slope and has been observed periodically since that time.

SOIL CONDITIONS

The borings revealed that the clay terrace was formed mostly of clay with some silty layers. Figure 8 is a boring log and a profile of test results. There are three major clay layers separated by silt layers a few inches thick. The top layer is hard grey clay with some red bands. It appears to be somewhat overconsolidated, probably due to weathering. From elevation 235 to elevation 220 the second, softer layer consists of stratified clay with some silt dustings between the layers. The liquidity index of this layer is close to unity. The lower layer (below elevation 220) consists of firm clay with a liquidity index well above one. Pore water salt concentration determinations indicated less than 1 gm per litre throughout the borings. Only the lower two layers of clay were involved in the landslide.

Field vane tests were conducted at two locations (Figure 3) and results from both holes are shown on Figure 8. Preconsolidation pressures determined from consolidation tests on 54 mm piston samples are also indicated on Figure 8.

GROUNDWATER OBSERVATIONS

The four piezometers installed after the landslide were located at the top of the slope. After one year, one piezometer, 0_1, was removed from the top and reinstalled at the toe of the slope. The location of the piezometers is indicated on Figure 3. The piezometers were installed at the following depths: 0_1 - 10 ft, 0_2 and 0_3 - 20 ft and 0_4 - 42 ft. Figure 9 gives the measured piezometric elevations with time. A substantial downward gradient of nearly 10 ft in 20 ft is indicated by piezometers 0_3 and 0_4. Piezometers 0_1 and 0_2, located close to the top of the scarp, were soon influenced by the presence of the slide crater.

Using the maximum readings recorded in 0_3, 0_4 and 0_1 (relocated), an approximate flow net was constructed. The slide surface was superimposed and an approximate average value of $r_u = 0.4$ was determined along the slide surface. Because of the downward gradient and the low permeability of the clay, it is conceivable that conditions approaching full hydrostatic pressure could exist for a shallow slip surface after a prolonged wet period.

STABILITY ANALYSIS

Since the failure surface could be determined with reasonable accuracy, there was a good opportunity to compare the measured shear strength with that computed from analysis. First an undrained analysis was made, using the undrained strengths measured by the field vane, but such an analysis proved unsatisfactory. The slide surface required only 350 psf of undrained shear strength, whereas the measured field vane strengths over the zone of failure was 1360 psf. This yielded an apparent factor of safety of 3.9.

Following the procedure outlined by Crawford and Eden (1), the required cohesion necessary for stability was computed for various values of φ' and r_u. The results of these computations are presented on Figure 10, and critical circles for $\varphi' = 5°$ and $\varphi' = 30°$ and $r_u = 0.59$ are shown on Figure 7. It will be noted that the actual failure surface is somewhat shallower, with its centre located at a point above the toe, than any of the critical circles derived from the computer analysis.

The studies with the computer also can define an envelope relating the average effective normal stress on the failure plane and the required shearing resistance (2). This envelope is presented in Figure 11, along with envelopes established by Kenney (3) for the Selnes and Breckenridge slides. Also plotted on Figure 11 are the average normal stress and the required undrained shear strength for the actual failure surface (Point 1). It plots well below the envelope.

SHEAR STRENGTH

Since the undrained analysis using results of the field vane test was obviously faulty, a comprehensive program of triaxial tests was conducted on some of the tube samples obtained at depths from 20 to 40 ft. Eight consolidated-undrained tests with consolidation pressure ranging from 3.00 to 6.00 kg/cm^2 were conducted to establish the Mohr envelope in the normally consolidated range. These tests were consolidated isotropically and strained at a rate of about 2 per cent per hour (Table 1).

In the working stress range, i.e. from no confining pressure up to the preconsolidation pressure, a series of triaxial drained tests were undertaken. Three types of drained tests were used, each yielding a different stress path. In the first series σ_1 was kept constant with decreasing σ_3. In the second series, σ_3 was held constant with increasing σ_1. The third series was conducted by keeping the average stress constant, i.e. $\left(\frac{\sigma_1 + \sigma_3}{2} = C\right)$.

Figure 12 is a plot of the stress paths of the tests. Tables II, III and IV are summaries of these tests.

Of the drained tests with σ_1 increasing, two results were considered unsatisfactory (148-17-5 and 148-17-8) because the stress levels were sufficient to cause large volume changes and the specimens could not be brought to a well-defined state of failure.

In trimming the specimens for the triaxial tests, curious fault-like structures were observed in some of the specimens, suggesting either fissures or pre-existing failure planes. Such specimens were closely observed during the test, and these discontinuities did not seem to influence the results obtained or the position of the eventual failure planes.

From the results of 15 drained tests at consolidation pressures less than 1.0 kg/cm^2, it is found that $\frac{\sigma_1' - \sigma_3'}{2} = 0.088 + \frac{\sigma_1' + \sigma_3'}{2} \tan 29.5°$. Using Bishop's (4) conversion,

$\frac{\sigma'_1 - \sigma'_3}{2} = d_o + \frac{\sigma'_1 + \sigma'_3}{2} \tan \Psi$ can be converted to the form

$S = C' + \sigma'_n \tan \varphi$ by $\tan \Psi = \sin \varphi'$ and $d_o = C' \frac{\tan \Psi}{\tan \varphi'}$.

In this case $\varphi' = 34.4°$ and $C' = 0.106$ kg/cm^2.

When all the triaxial results are considered, it appears that there are three distinct behaviour zones for the clay on this site. At low confining pressures, a brittle nearly elastic behaviour is evident. Drained tests at a constant rate of strain exhibited a peak followed by a significant drop. At consolidation pressures between 1.0 and the preconsolidation pressure, a complex behaviour pattern was evident. Tests 148-17-5 and 148-17-8 are typical of this behaviour. Figure 12 indicates the strain at various stages and it is evident that in later stages a work-hardening process was occurring, with associated large volume changes. In the normally consolidated range, a work-hardening process begins at low stress levels.

CONCLUSIONS

To conduct a stability analysis, information on three factors is necessary: (a) the geometry of the slope, including the failure plane, (b) the groundwater conditions and (c) the effective shear strength of the soil along the failure surface. With the Orleans slide, the geometry was reliably known. Less knowledge was available concerning the groundwater conditions and the shear strength.

From the piezometric observations, the highest average r_u is about 0.4. Because of the downward gradient and the shallow depth of the slide surface, it is conceivable that with a prolonged rainfall, conditions could temporarily approach that of full hydrostatic pressure.

Assuming that the failure surface was correctly determined and that piezometric conditions were close to full saturation (r_u = 0.59), the following may be concluded:

1. The shear strength measured with the field vane is much higher than required for stability. The failure conditions applied to the soil by the field vane do not appear to be relevant to a slope failure which, in cases such as the landslide at Orleans, occurs in the overconsolidated range of Leda clay.

2. The computer analysis indicated a higher strength required for stability than that actually mobilized along the failure surface. No allowance was made in the computer studies for tension cracks or anisotropic effects in the soil. The actual failure surface was somewhat shallower, with its centre displaced towards the toe, than the critical circles determined by the computer analysis. The actual failure surface was reasonably circular. It is possible that imperfections such as fissures or anisotropic properties of the clay, or strain incompatibility along the failure surface, influenced the position of the failure surface.

3. Drained triaxial tests conducted within the range of effective stresses along the actual failure surface yielded shear strengths which were consistent with those calculated for an ideal slope. Three distinct types of behaviour were evident in the triaxial tests: a brittle type of failure at low strains at low confining pressures, an elastic behaviour changing to one of work-hardening at intermediate stresses, and a work-hardening behaviour in the normally consolidated range. In the case of the Orleans slope, only the brittle type of failure is relevant.

Since this is one example only of a slope failure in Leda clay, the apparent agreement may be fortuitous. Studies of other well-documented case records are required before firm conclusions can be drawn.

REFERENCES

1. Crawford, C. B. and W. J. Eden. Stability of natural slopes in sensitive clay. Proc. A. S. C. E. Jour. Soil Mechanics and Foundation Engineering, Vol. 93, No. SM4, July 1967, p. 418-436.

2. Kenney, T. C. Slide behaviour and shear resistance of a quick clay determined from a study of the landslide at Selnes, Norway. Proc. Geotechnical Conference, Oslo, Vol. 1, 1967, p. 57-64.

3. Kenney, T. C. Discussion to Stability of natural slopes in sensitive clay by C. B. Crawford and W. J. Eden. Proc. A. S. C. E. Jour. Soil Mechanics and Foundation Engineering, Vol. 94, No. SM5, 1968, p. 1185-1190.

4. Bishop, A. W., I. Alpan, G. E. Blight and I. B. Donald. Factors controlling the strength of partly saturated cohesive soils. Proc. Research Conference on Shear Strength of Cohesive Soils, A. S. C. E., 1960, p. 503-532.

TABLE I

SUMMARY OF UNDRAINED TRIAXIAL TESTS

Sample No.	Elevation, ft	Water Content, %		σ'_c, kg/cm^2	$\sigma'_1 - \sigma'_3$ (max), kg/cm^2	$\Delta\mu_f$, kg/cm^2	σ'_{3f}, kg/cm^2	ϵ_f, %	Rate of Strain, %/hr	$\frac{\sigma'_1+\sigma'_3}{2}$, kg/cm^2	$\frac{\sigma'_1-\sigma'_3}{2}$, kg/cm^2
		Init.	Final								
148-12-7	231.4	61.9	48.1	3.00	1.57	1.73	1.27	1.9	2	2.055	0.785
148-12-8	230.9	62.4	45.1	4.02	2.17	2.33	1.69	2.1	2.2	2.775	1.085
148-12-9	230.5	66.4	44.4	5.01	2.83	2.92	2.09	2.2	1.9	3.505	1.415
148-12-10	230.3	67.7	43.0	6.01	3.60	2.85	3.16	2.2	1.9	4.960	1.80
148-18-7	213.3	70.8	49.7	4.02	2.46	2.16	1.86	1.9	2.1	3.090	1.23
148-18-8	212.9	67.1	51.2	3.01	1.59	1.72	1.29	2.1	2.1	2.065	0.795
148-18-9	212.5	70.3	46.2	5.02	3.08	2.28	2.74	1.9	2.1	4.280	1.54
148-18-10	212.3	71.6	44.7	6.02	3.63	3.14	2.88	1.7	2.1	4.695	1.825

TABLE II

SUMMARY OF DRAINED TRIAXIAL TESTS - σ_3' DECREASING (STEP LOADING)

Sample No.	Elevation, ft	Water Content, %		σ_c', kg/cm^2	$\sigma_1'-\sigma_3'$ (max), kg/cm^2	σ_{3f}', kg/cm^2	ϵ_f, %	Time to Failure, Last increment	Duration of Test, days	$\frac{\sigma_1+\sigma_3}{2}f$, kg/cm^2	$\frac{\sigma_1-\sigma_2}{2}f$, kg/cm^2
		Init.	Final								
148-16-4	220.0	67.0	68.8	0.85	1.26	0.05	0.5	7 hr	16	0.65	0.60
148-16-5	219.7	66.5	66.0	1.70	1.34	0.20	1.0	50 hr +	9	0.87	0.67
148-16-7	219.2	65.3	61.0	2.00	1.445	0.60	6.7	10 min	20	1.322	0.72
148-20-2	208.4	66.7	65.1	1.00	0.85	0.15	1.26	8 hr	15	0.575	0.425
148-20-5	207.7	70.4	70.6	1.00	0.96	0.05	0.28	72 hr +	6	0.53	0.48

TABLE III

SUMMARY OF DRAINED TRIAXIAL TESTS - σ_1' INCREASING

Sample No.	Elevation, ft	Water Content, %		σ_c' kg/cm^2	$(\sigma_1'-\sigma_3')$ max. kg/cm^2	σ_{3f}', kg/cm^2	ϵ_f, %	Rate of Strain, %/hr	Duration of Test	$\frac{\sigma_1+\sigma_3}{2}f$, kg/cm^2	$\frac{\sigma_1-\sigma_3}{2}f$, kg/cm^2
		Init.	Final								
148-17-4	217.0	73.0	72.0	0.60	1.30	0.60	1.47	0.22	6.75 hr	1.25	0.65
148-17-5	216.7	75.0	71.7	1.54	0.984	1.54	1.40	0.17	8.15 hr	1.992	0.492
148-17-7	216.3	74.0	72.9	0.30	0.80	0.30	1.00	0.23	4.42 hr	0.70	0.40
148-17-8	215.8	70.6	65.2	1.00	1.484	1.00	5.80	0.19	31 hr	1.742	0.742
148-16-10	218.2	73.4	73.4	0.15	0.49	0.15	0.50	0.50	1 hr	0.395	0.245
148-17-9	215.5	--	--	--	0.53	-	0.85	0.41	2.08 hr	0.265	0.265
148-20-4	208.0	69.3	68.3	0.25	1.60	0.25	1.25	Step loading	40 days	1.05	0.80
148-20-8	206.9	68.5	-	0.05	0.55	0.05	0.40	Step loading	4 days	0.325	0.275

TABLE IV

SUMMARY OF DRAINED TRIAXIAL TESTS - $\frac{\sigma_1 + \sigma_3}{2}$ CONSTANT

Sample No.	Elevation, ft	Water Content %		σ'_c, kg/cm^2	σ_{3f}, kg/cm^2	ϵ_f, %	Time to Failure, Last increment	Duration of Test	$(\sigma_1 - \sigma_3)f$, kg/cm^2	$\frac{\sigma_1+\sigma_3}{2}$, kg/cm^2	$\frac{\sigma_1-\sigma_3}{2}$, kg/cm^2
		Init.	Final								
148-24-2	217.3	71.3	73.5	0.40	0.05	2.75	25 min	29 hr	0.677	0.39	0.34
148-24-3	217.0	68.2	69.8	0.20	0.00	0.40	12 min	25 hr	0.395	0.20	0.20
148-24-4	216.7	68.7	70.8	0.20	0.00	2.68	34 min	24 hr	0.381	0.19	0.19
148-25-1	215.7	68.1	68.0	0.80	0.35	0.75	21 min	40 hr	0.898	0.799	0.449
148-25-2	215.4	68.9	69.1	0.60	0.15	0.71	2 hr +	5 days	0.898	0.60	0.45
148-25-3	215.0	68.1	69.0	0.30	0.00	0.47	23 min	40 hr	0.40	0.30	0.20
148-25-4	214.7	69.2	68.3	1.00	0.30	1.45	15 min	7 days	1.395	1.00	0.70
148-25-6	214.0	68.3	68.3	0.40	0.15	2.8	74 min	3 days	0.486	0.40	0.243
148-25-5	214.4	65.3	66.4	0.40	0.10	1.4	Cont. loading	34 hr	0.806	0.50	0.403
148-24-5	216.4	66.6	65.7	0.80	0.43	1.7	Cont. loading	51 hr	1.36	1.11	0.68

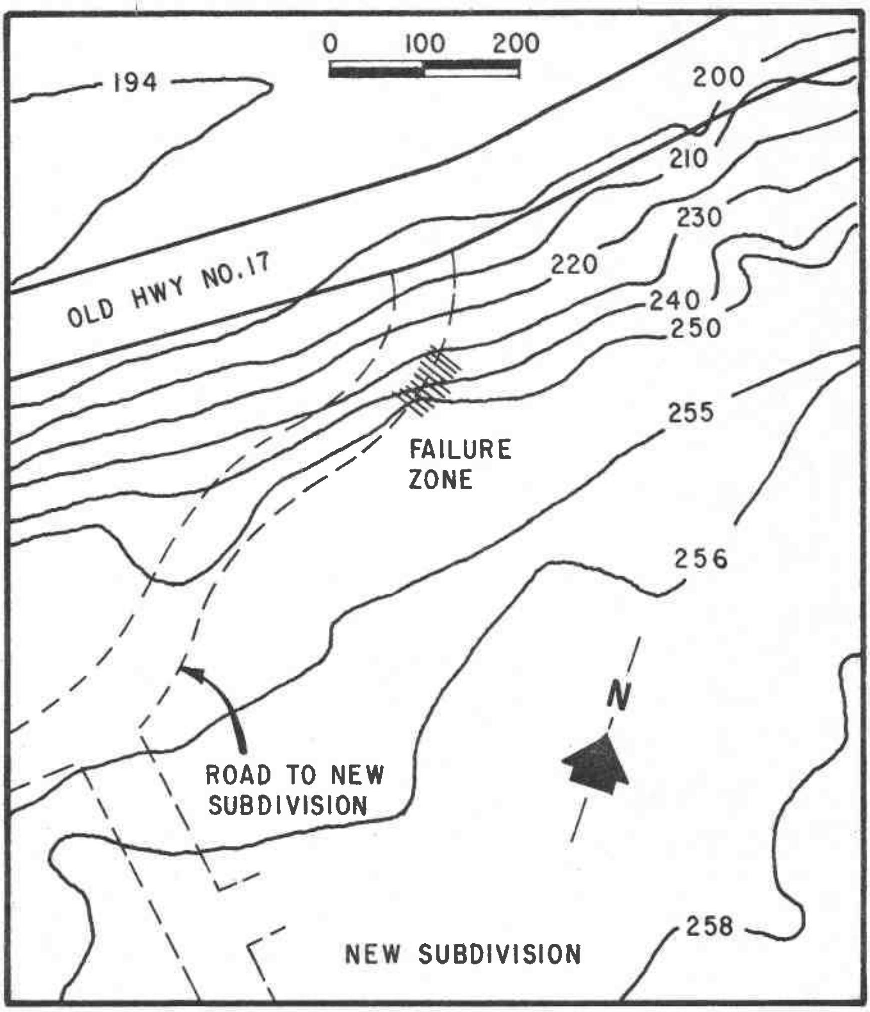

FIGURE 1

SLIDE AREA BEFORE THE DEVELOPMENT

BR 4219-1

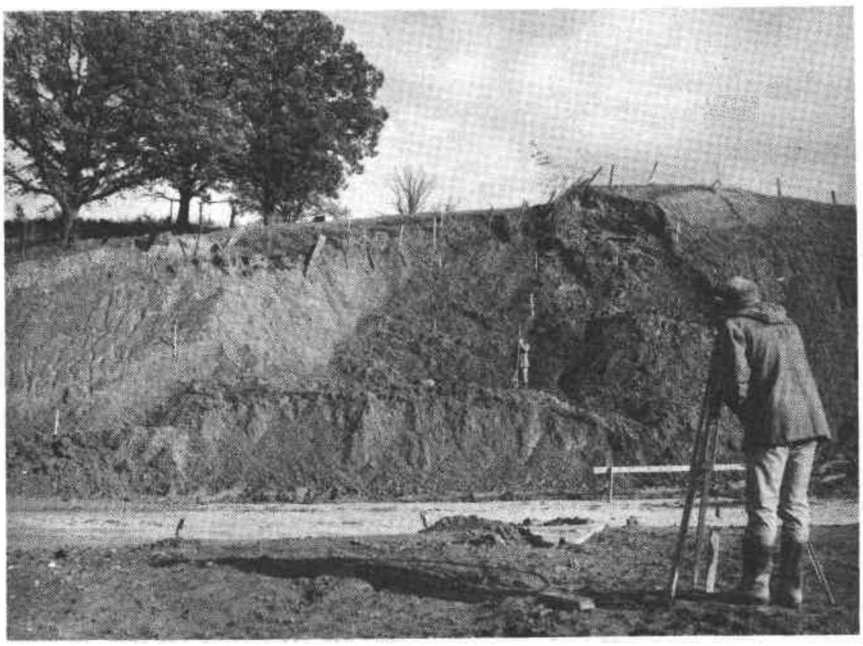

Figure 2

View of crater of first slide

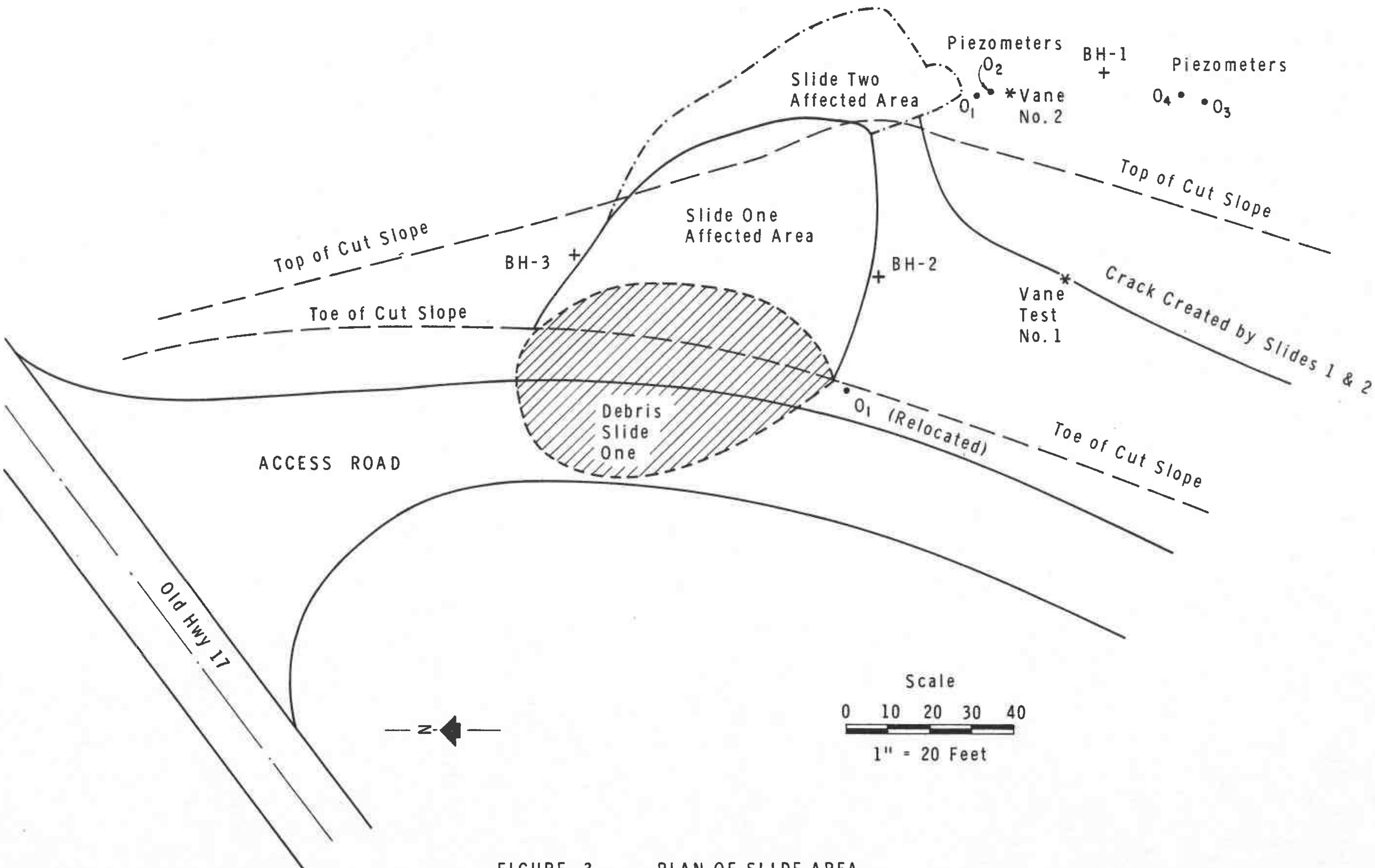

FIGURE 3 PLAN OF SLIDE AREA

884219-2

Figure 4

Tension cracks preceding second slide

Figure 5

Crater after second slide

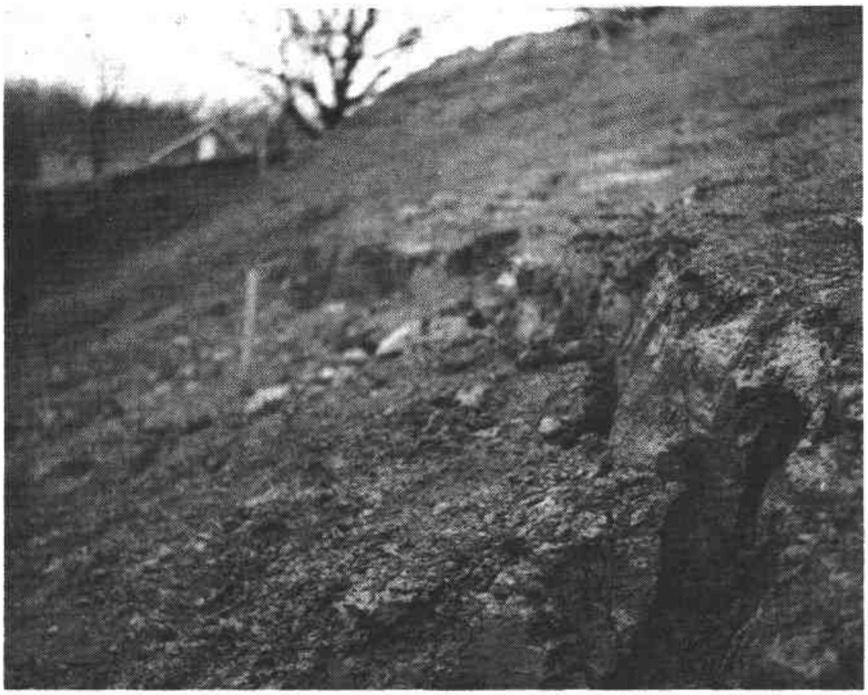

Figure 6

Tension cracks right of crater

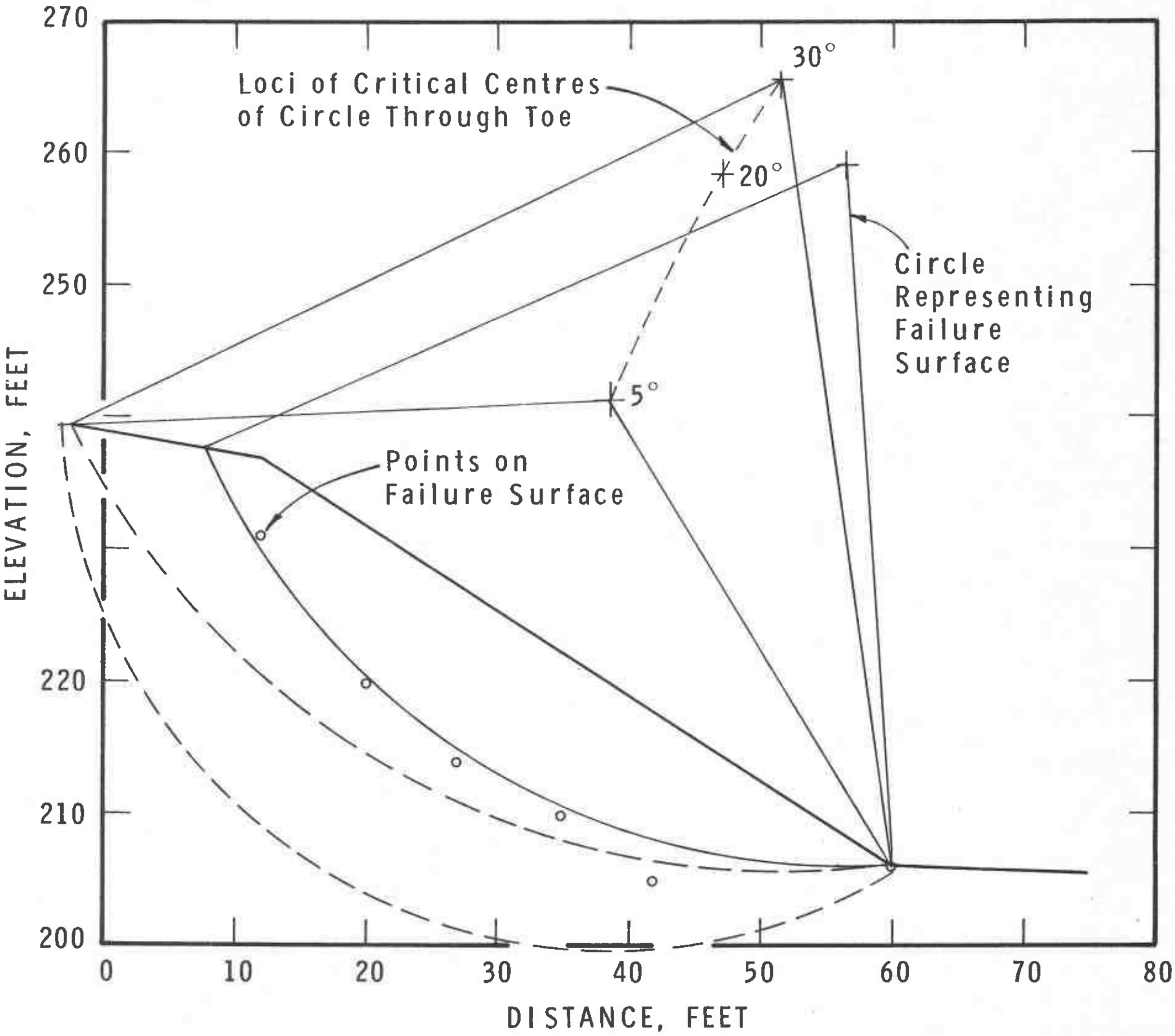

FIGURE 7 PROFILE OF ORLEANS SLOPE

BR 4219-3

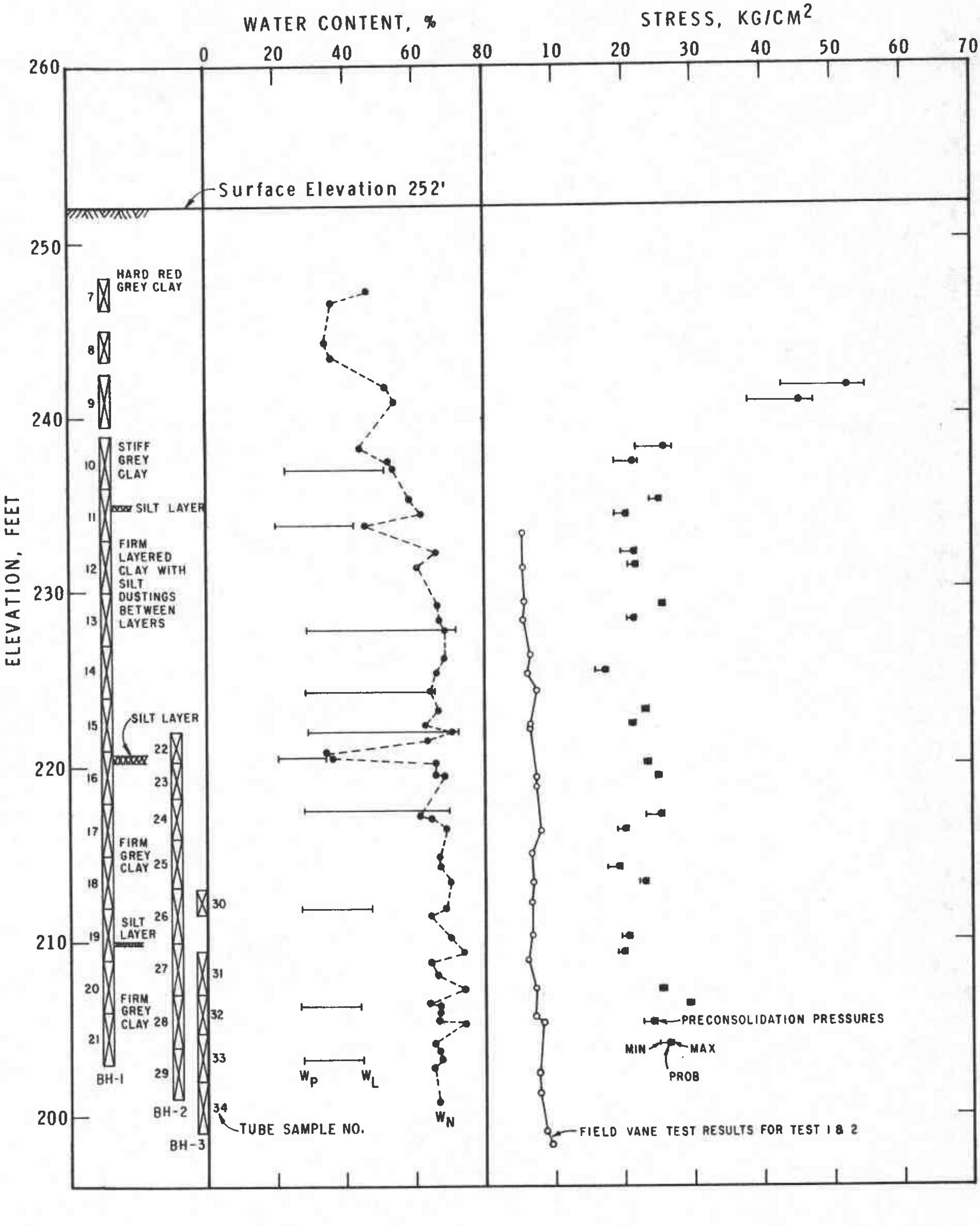

FIGURE 8

BORING LOG & TEST RESULTS - ORLEANS SLIDE

BR 4219-4

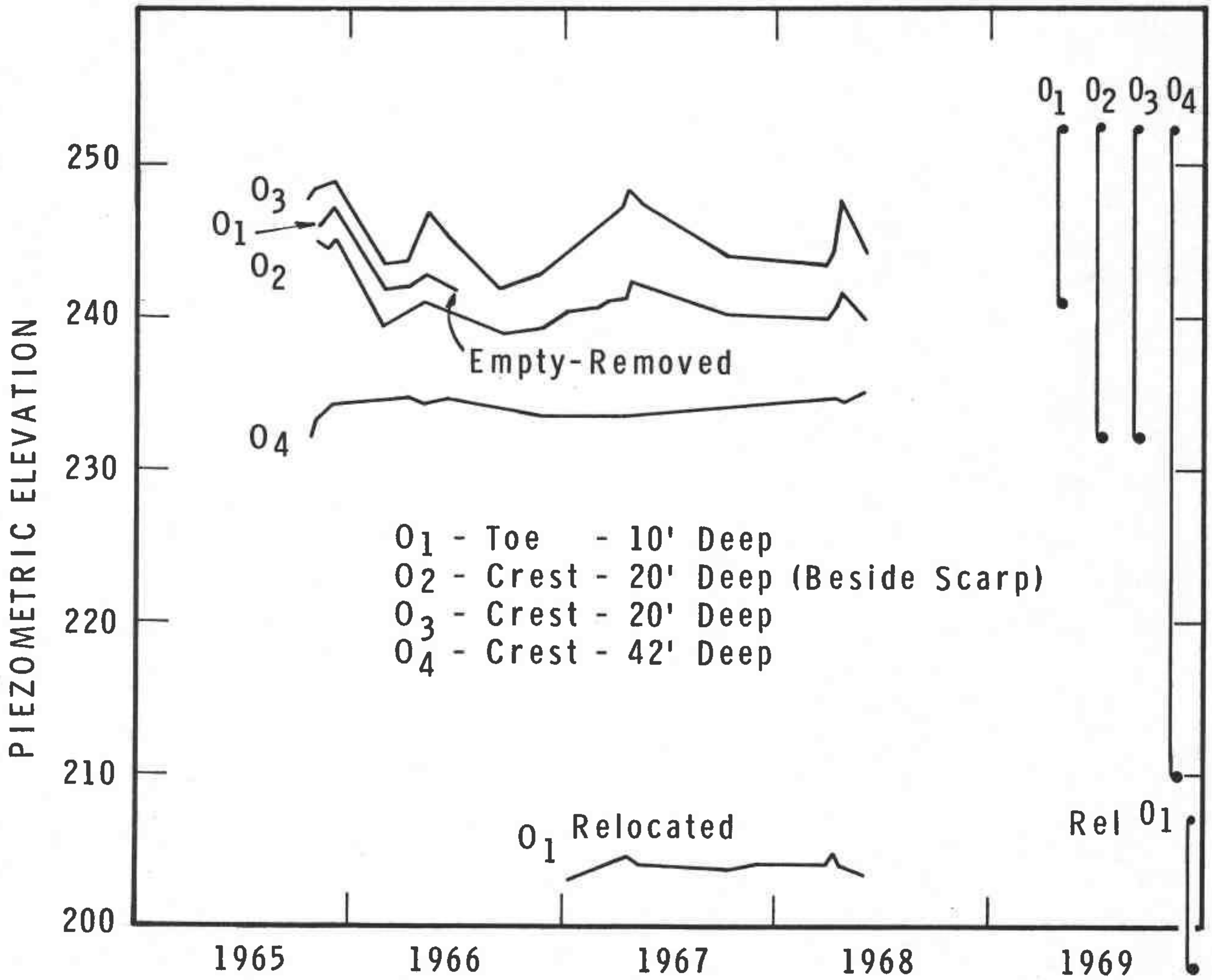

FIGURE 9

VARIATION OF PIEZOMETRIC ELEVATIONS

BQ 4219-5

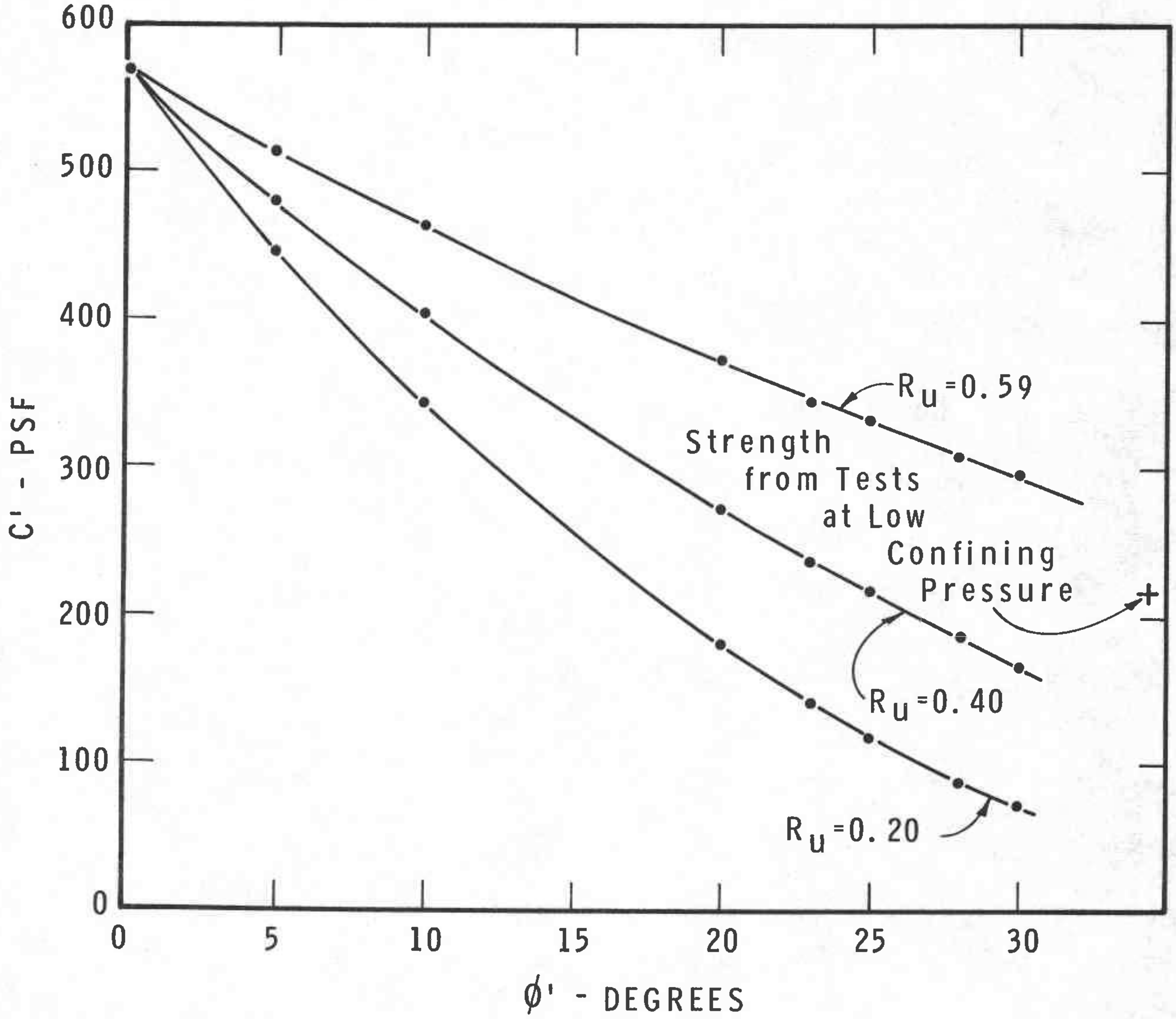

FIGURE 10

ORLEANS SLOPE STRENGTH REQUIRED FOR STABILITY

BQ 4219-6

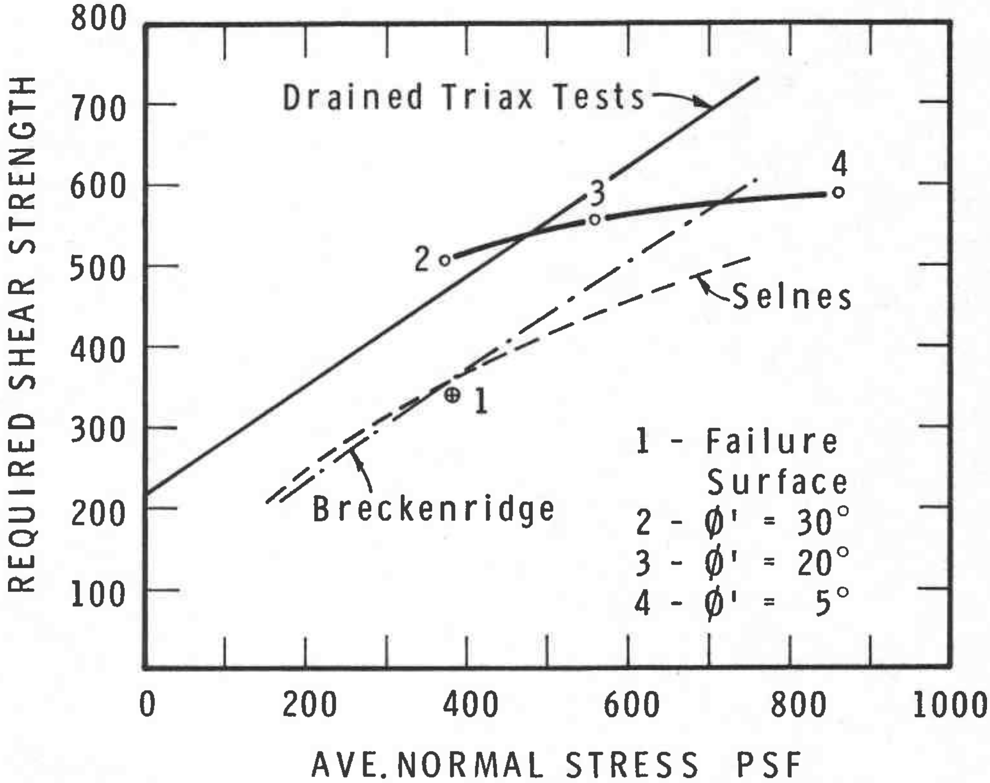

FIGURE 11

CRITICAL STRESS CURVE FOR ORLEANS SLIDE

BQ 4219-7

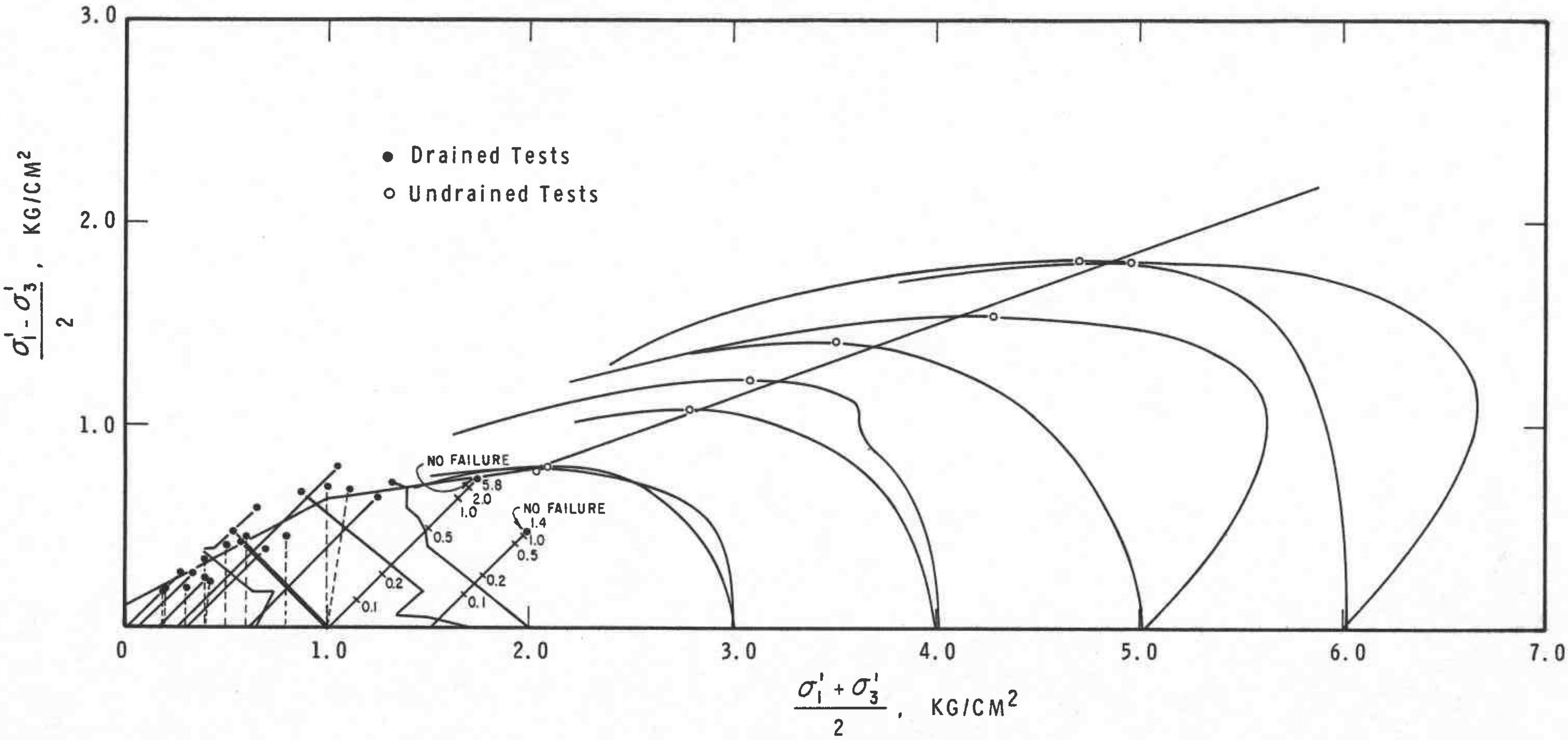

FIGURE 12 STRESS PATHS FOR TRIAXIAL TESTS

BR 4219-8